DOI: https://doi.org/10.24425/amm.2025.154459

SOO-HO JUNG¹, JINHEE BAE¹, JIHUN YU¹, KYUNG TAE KIM^{1*}

ELECTROSTATIC REACTIVITY CONTROL OF POLYTETRAFLUOROETHYLENE-COATED ALUMINUM POWDERS USING ANTISTATIC AGENTS

Aluminum (Al) powders are coated by polytetrafluoroethylene (PTFE), which replaces the naturally formed oxide layer, enhancing thermal oxidation performance via simultaneous exothermic reactions doubling exothermic enthalpy energy compared to uncoated Al powder. However, the PTFE coating significantly increases electrostatic charge, raising ignition risks. The incorporation of antistatic agents such as Bis-Hydroxyethyl Cocomonium Nitrate within a glycerol solution produced a 61% reduction in the electrostatic charge due to surface charge modification of the powders. This study demonstrates the potential of PTFE in enhancing combustion while addressing electrostatic hazards, ensuring safer handling. The findings shows the way for optimized PTFE/Al powder in energetic applications.

Keywords: Aluminum powder; PTFE coating; Static electricity; Antistatic agent

1. Introduction

Since aluminum (Al) powder is widely known for its high energy release per unit mass during combustion, it is considered as a promising material in the field of energetic applications including propellants, pyrotechnics, and explosives [1-4]. However, the thermal oxidation behavior of aluminum powder is often hindered by the densely packed surface oxide layer, which limits oxygen diffusion from the external atmosphere and results in incomplete combustion that is lower than theoretically expected. This phenomenon reduces the overall heat energy output and even leaves substantial aluminum residues post-combustion.

To address this limitation, fluorine-based polymers such as polytetrafluoroethylene (PTFE) and polyvinylidene fluoride (PVDF) have been investigated as potential coating materials to replace the naturally formed aluminum oxide layer [1-3,5]. In particular, the fluorine-rich structure of PTFE facilitates enhanced combustion by minimizing the barrier to oxygen diffusion, thereby allowing for more complete oxidation and higher thermal energy output due to simultaneous reactions between Al-O and Al-F. Differential Scanning Calorimetry (DSC) analysis in our previous studies indicate that the PTFE-coated Al powder demonstrates significantly higher exothermic activity compared to uncoated Al powder, with an observed doubling of heat release regardless of powder size [2,5,6].

The PTFE coating clearly enhances the heat-generating capacity of Al powder; however, the electrostatic charges formed on the powder surface, which are crucial from the viewpoint of a practical application, have not been investigated. In general, PTFE is widely used as an electron acceptor in triboelectric generators due to its easy frictional electrification. Therefore, studying the formation of electrostatic charges on the PTFE/Al powder is essential [7,8]. Preliminary tests indicated that the PTFE/Al powder exhibits up to a 20-fold increase in electrostatic charge compared to that of uncoated Al powder. This necessitated the addition of antistatic agents to improve handling safety. In order to mitigate this electrostatic hazard, we investigated two different antistatic agents, focusing on compounds that are both effective in static charge reduction and safe for human contact [9-18]. Glycerol and Bis-Hydroxyethyl Cocomonium Nitrate were selected based on their hygroscopic properties and compatibility with PTFE-coated powder [10,15,19]. These agents were incorporated into the PTFE/Al powder via a mixing process. Notably, the addition of Bis-Hydroxyethyl Cocomonium Nitrate in a glycerol-diluted solution achieved a 61% reduction in static charge due to the formation of a thick conductive surface layer. Thus, this study explores the both the benefits and challenges of PTFE/Al powder for practical use, presenting a solution to enhance combustion efficiency while addressing electrostatic risks through effective antistatic treatments.

^{*} Corresponding author: ktkim@kims.re.kr



¹ NANO MATERIALS RESEARCH DIVISION, KOREA INSTITUTE OF MATERIALS SCIENCE, 797 CHANGWONDAERO, SEONGSAN-GU, CHANGWON, GYEONGNAM 51508, REPUBLIC OF KOREA

2. Experimental

A PTFE dispersion of 60 g was diluted with distilled water to achieve a 20 wt.% concentration and stirred at 80°C for over 30 minutes. Separately, a 1 wt.% hydrofluoric acid (HF) solution of 1200 g was prepared for the aluminum powder coating process, and 100 g of 35 μ m Al powder was added. Upon addition, heat and bubbles formed due to the dissolution reaction of the aluminum surface oxide layer, and the bubble production stabilizing within 2 minutes. Next, the diluted PTFE dispersion was added to the HF solution, and the mixture was stirred for 30 minutes to allow the coating reaction to proceed thoroughly. The slurry was then filtered to recover the synthesized PTFE/Al powder, which was initially dried in a vacuum oven at 60°C for 24 hours, followed by heat treatment in a box furnace at 300°C for 30 minutes.

Thermogravimetic analysis (TGA) and Differential scanning calorimetry (DSC) results were obtained by the experimental condition of heating rate of 10°C/min up to 1400°C under air atmosphere (Model: Discovery SDT 650, TA instrument). TGA and DSC of both powders produce the information of thermal oxidation behavior

To impart antistatic properties to the PTFE/Al powder, two types of antistatic solutions were prepared as follows: a 10 wt.% glycerol aqueous solution and a 5 wt.% glycerol solution with an additional 0.05 wt.% of Bis-Hydroxyethyl Cocomonium Nitrate. The synthesized powder was introduced into the prepared solutions and stirred for 30 minutes. The powder was then dried

in a vacuum oven at 60°C for 24 hours, after which the electrostatic force was measured. Electrostatic force measurements were conducted using a powder flow analyzer (Model: Revolution Powder Analyzer, Mercury Scientific Inc.).

3. Results and discussion

Fig. 1 shows SEM images and powder size distribution of both Al powder and PTFE/Al powder. Fig. 1a displays information of surface morphologies and cross-sectional SEM images including EDS result of one uncoated Al powder. Average powder size of the Al powder used in this study was measured as 35 µm (D₅₀) as shown in Fig. 1b. The PTFE coating layer was clearly visible in the cross-sectional SEM image of PTFE/Al powder in Fig. 1c. The thickness of the PTFE layer was measured to be approximately 150 nm. This study used 35 µm Al powder for the demonstration of oxidation reaction and the electrostatic properties. Fig. 1d shows powder size distribution of PTFE/Al powder, in which D₁₀, D₅₀, and D₉₀ of the powder were 19.83, 32.86, 56.12 µm, respectively. The particle size of the PTFE/Al powder decreased slightly after coating; D_{10} , D_{50} , and D_{90} were 17.71, 28.35, 46.05 μm, respectively. As a result, a slight decrease in particle size was observed, with the D₅₀ value reduced by approximately 4 µm. Since the coating thickness of PTFE is greater than that of the aluminum oxide layer, the minor reduction in particle size is presumed to be due to excessive dissolution caused by acid during the coating process.

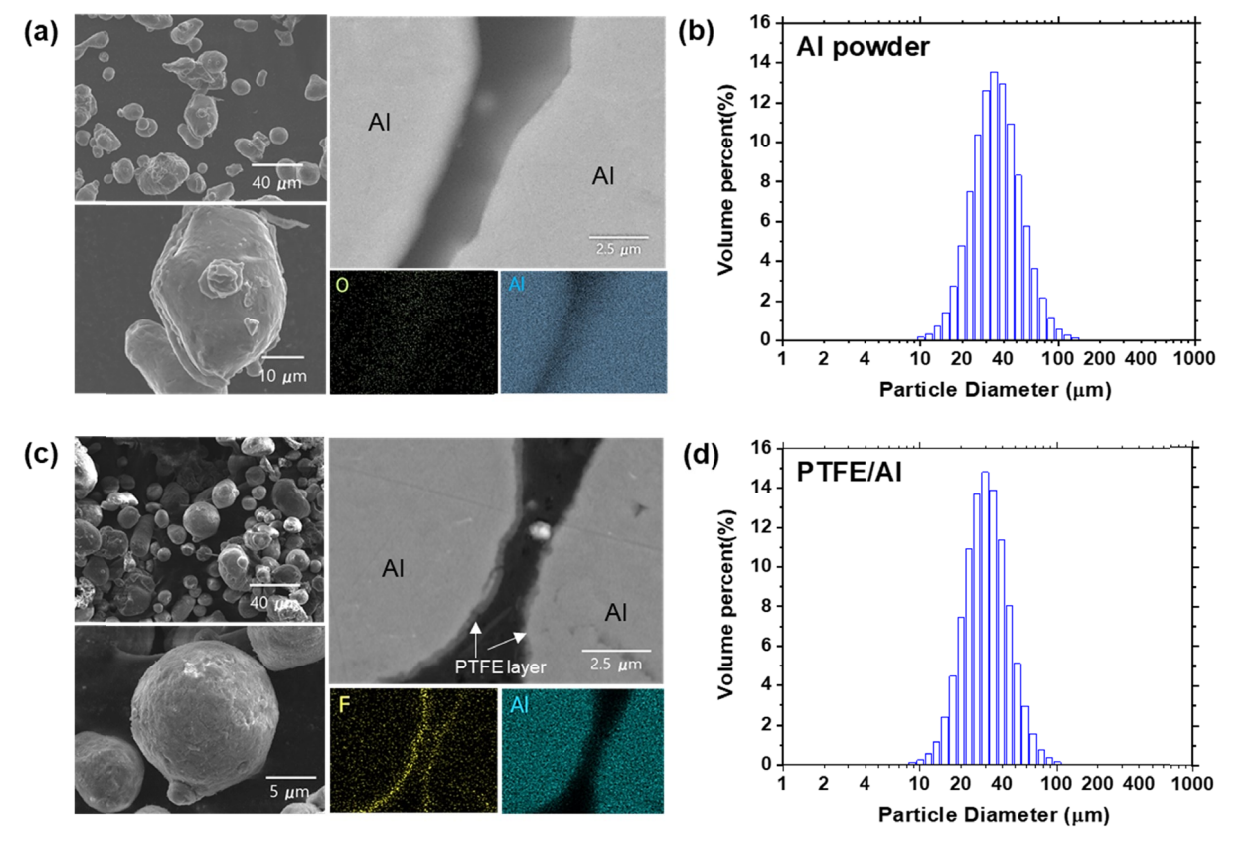


Fig. 1. SEM images and the powder size analysis result. (a) Shape, cross section image and EDS result of the Al powder, (b) powder size analysis of Al powder, (c) shape, cross section image and EDS result of the PTFE/Al powder, and (d) Powder size analysis of PTFE/Al powder

Fig. 2a compares the weight changes as a function of temperature for both uncoated Al powder and PTFE/Al powder. Figs. 2b and 2c show DSC results displaying heat flow as a function of temperature of uncoated Al and PTFE/Al powders. Aluminum powder increased by 112.57%, while the weight of PTFE/Al powder increased by 130.14%, indicating that a greater amount of aluminum was oxidized. The PTFE coating acts as an additional oxidizing agent, contributing to additional heat generation during the oxidation of aluminum powder [4].

The increase in heat generation is verified through DSC analysis, showing three primary peaks. The first peak at ~610°C corresponds to the oxidation of the Al powder surface, the second endothermic peak at ~650°C results from aluminum liquefaction, and the main exothermic peak occurs between 800-900°C, continuing to ~1100°C due to the oxidation of liquefied aluminum. When the exothermal enthalpy energy of aluminum powder was 459.9 J/g, the PTFE/Al powder exhibited an increased exothermal enthalpy energy of 940.1 J/g. (Fig. 2d) The exothermal enthalpy energy increased by 204%, as a result of the coating.

The PTFE/Al powder exhibits relatively higher heat generation compared to uncoated Al powder with a similar average particle size. In the case of Al powder, a dense oxide layer naturally forms on the surface, which thickens as oxidation progresses with increasing temperature. During combustion, this oxide layer tends to impede the oxidation reaction, leading to incomplete combustion of Al core. Therefore, heat genera-

tion was lower than expected. On the contrary, in the case of Al powder where the oxide layer is replaced by PTFE, fluorination leading to AlF₃ formation preferentially occurs compared to the surface passivation effect by oxidation. Consequently, combustion proceeds continuously rather than being stopped by surface oxide, increasing heat energy.

Especially for Al powder, spontaneous combustion can occur in ambient air under specific conditions. Among these, spontaneous combustion could be triggered by electrostatic sparks, making it necessary to measure the electrostatic force of PTFE/Al powder. Electrostatic force was measured using an electrostatic charge measurement device, an accessory of the powder flow analyzer. By loading powder samples into a cylindrical drum and observing the change in charge over a set time and rotation speed, the electrostatic force can be measured (Fig. 3a). Fig. 3b shows the electrostatically measured voltage as a function of time for the uncoated Al powder, PTFE/Al powder and PTFE/Al powder treated with two different types of antistatic agents. Since the absolute value of the electrostatic force can vary depending on the measurement conditions, we compared the relative electrostatic force between PTFE/Al powder and Al powder. The results showed that PTFE/Al powder exhibited approximately 20 times higher electrostatic force than Al powder, indicating a relatively lower safety level during storage and the need for improvement. To decrease the electrostatic force, the antistatic agent solution was applied by simply mixing the solution with

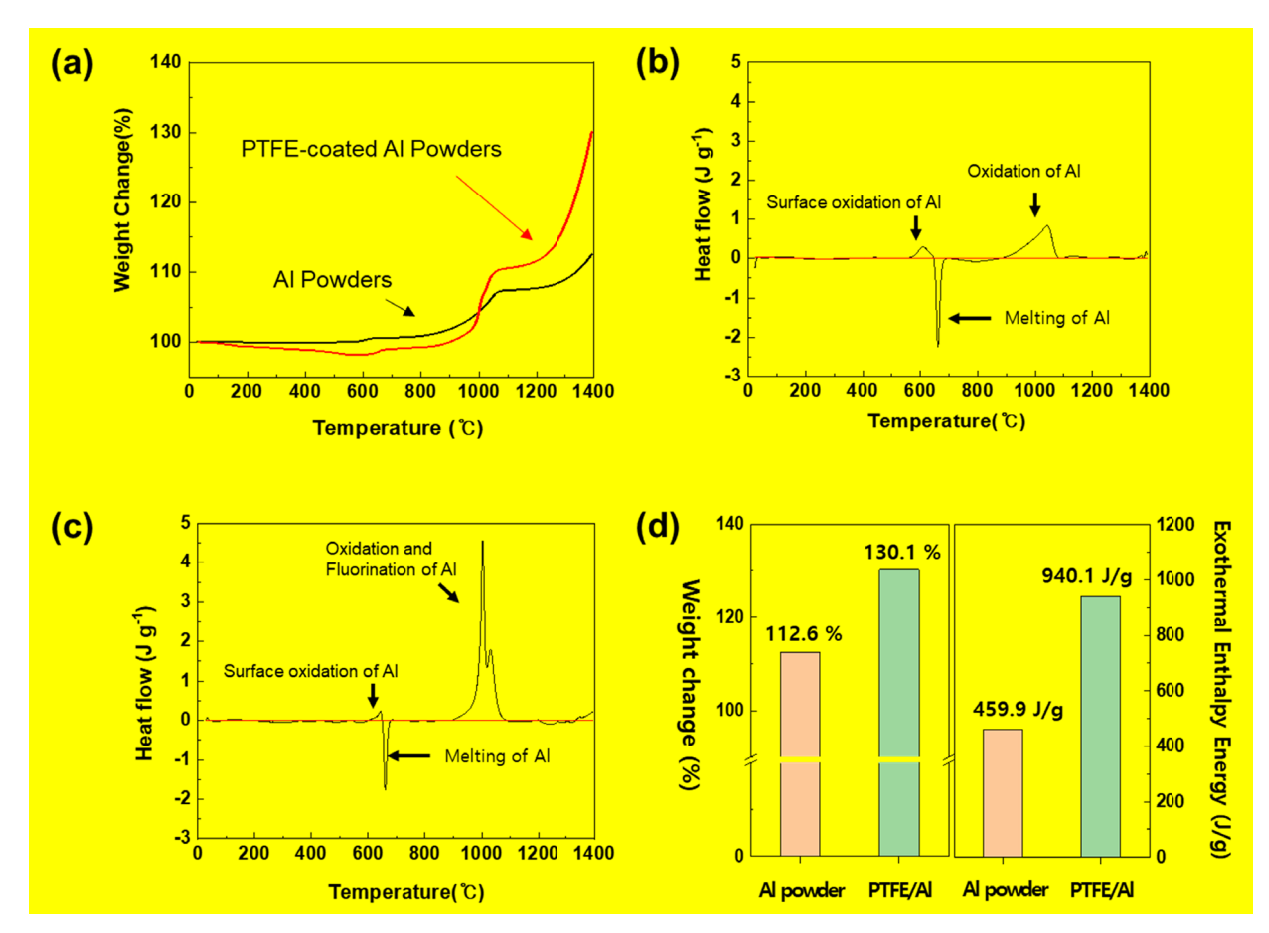


Fig. 2. TGA/DSC analysis results. (a) TGA results of Al and PTFE/Al powders, (b) DSC result of Al powder, (c) DSC result of PTFE/Al powder, and (d) total summary of TGA and DSC results. Labeled value of DSC results indicates the oxidation energy of the main peak

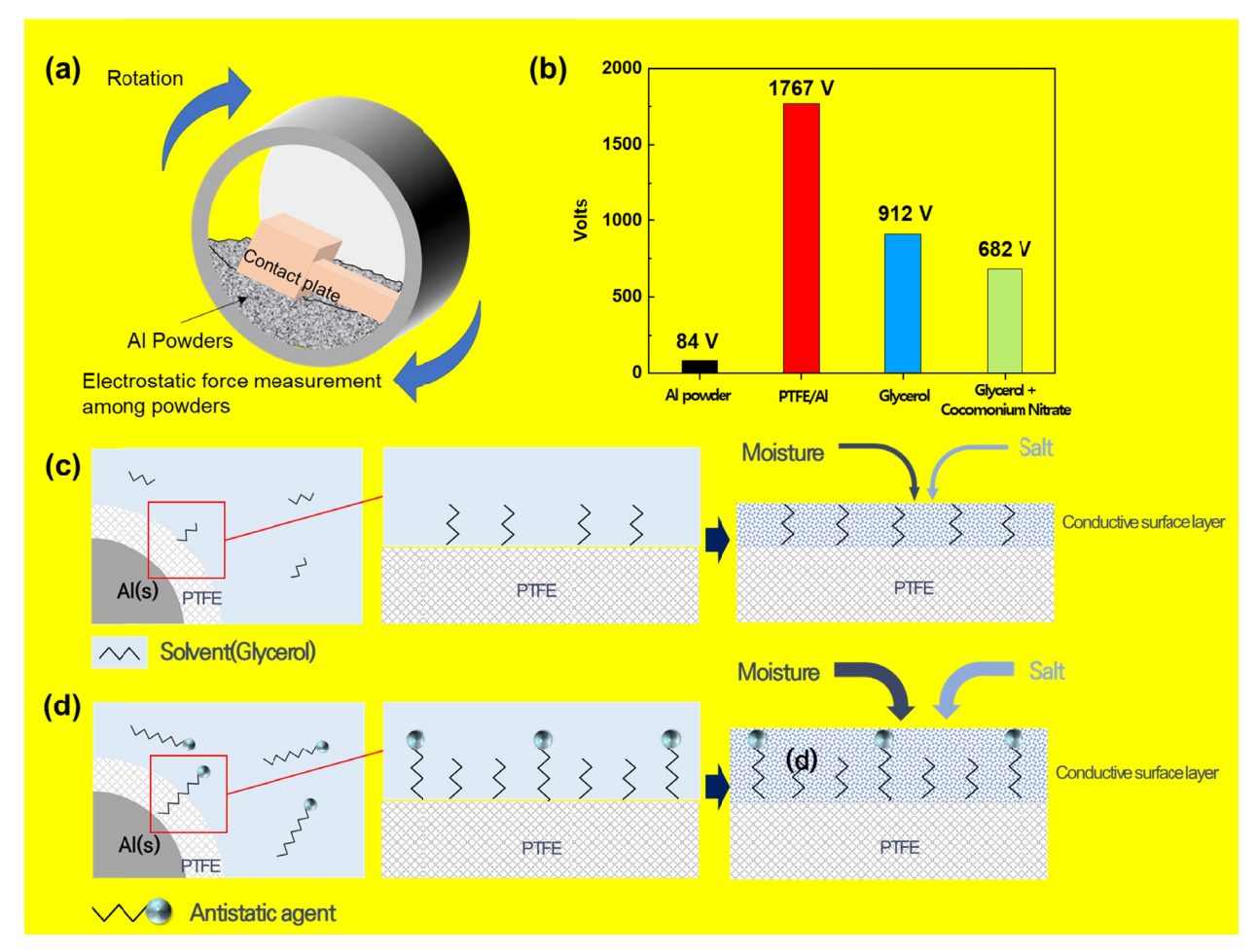


Fig. 3. Electrostatic charge test methods and the scheme of the antistatic agent working mechanism. (a) Scheme of the electrostatic charge measuring method: The sample drum is rotated at a programmed velocity and the charge of the contact plate is measured at programmable intervals. (b) Measured electrostatic voltage of four types of powders after 1 minutes of drum rotation. (c) Scheme of the glycerol on PTFE/Al powder, and (d) scheme of the glycerol and Bis-Hydroxyethyl Cocomonium Nitrate(Spray) on PTFE/Al powder

the powder. (Fig. 3c). As in TABLE 1, various surfactants with static-elimination properties have been reported, and from these, a safe and effective option for aluminum powder was selected. If the target has surface resistivity in the range of 10^9 to 10^{13} Ohms, it is considered antistatic. On the other hand, a sample having surface resistivity over 10^{14} Ohms is considered insulative.

Compared to the initial electrostatic force of PTFE/Al powder, treatment with glycerol achieved a 50% reduction, while the addition of a small amount of Bis-Hydroxyethyl Cocomonium Nitrate to glycerol resulted in a 61% reduction. Notably, even a minimal addition of Bis-Hydroxyethyl Cocomonium Nitrate (0.05 wt%) to the glycerol solution was sufficient to further decrease the electrostatic force effectively. Glycerol is an organic compound with three hydroxyl(-OH) groups. Due to the abundance of hydroxyl groups, it exhibits high hydrophilicity, providing moisturizing effects, and is safe for human use, making it a key ingredient in cosmetics. After brief mechanical mixing, residual glycerol on the PTFE/Al surface absorbs trace moisture from the atmosphere. The absorbed moisture includes trace amounts of salt, forming a conductive surface layer that reduces electrostatic force (Fig. 3c). Therefore, even a diluted glycerol solvent alone can effectively reduce electrostatic force.

TABLE 1 Examples of antistatic agents

Classifications	Antistatic agents	Resistivity	Ref.
Surface modifier agents (Ionic liquids)	[BMIM][PF ₆]	$1.52 \times 10^7 \Omega \cdot \text{cm}$	[16]
	[C ₄ mim][Tf ₂ N]	9.4×10 ¹¹ Ω·cm	[13]
	[C ₁₄ mim]Br	$2.60 \times 10^7 \Omega \cdot \text{cm}$	[9]
	[N ₄₄₄₁][Tf ₂ N]	$8.00 \times 10^7 \Omega \cdot \text{cm}$	[18]
Electrically conductive pillars	rGO	4.0×10 ¹⁰ Ω⋅cm	[20]
		$1.0 \times 10^2 \Omega \cdot \text{cm}$	[14]
		10 ⁶ Ω⋅cm	[21]
	MWCNTs	10 ⁸ Ω⋅cm	[19]
		10 ⁸ Ω⋅cm	[22]
		1.5×10 ⁷ Ω⋅cm	[17]
	СВ	10 ² Ω⋅cm	[12]
		6.8×10 ³ Ω⋅cm	[23]
		1.6×10 ⁶ Ω⋅cm	[11]
Conductive polymers	Polyaniline	3.2×10 ⁵ Ω·cm	[24]
Natural agents	Glycerol*	4.5×10 ¹⁰ Ω·cm	[10]
	Bis-Hydroxyethyl Cocomonium Nitrate	$10^9 \sim 10^{10} \Omega \cdot \text{cm}$	[25]

^{* 5} wt.% addition of glycerol to the target (Polystyrene)

To achieve additional electrostatic reduction, a small amount of Bis-Hydroxyethyl Cocomonium Nitrate was added to the diluted glycerol solution. This compound, derived from coconut oil, acts as an antistatic agent and is also safe for use in products designed to reduce static in hair. It features typical antistatic characteristics including a quaternary ammonium salt and a nitrate (NO₃) group, exhibiting higher polarity than glycerol. As a result, even with half the amount of glycerol and the addition of only 0.05 wt.% of the antistatic agent, further reduction in electrostatic charge was achieved. This is attributed to the increased absorption of moisture and salt due to its higher polarity, reducing the resistivity of the conductive surface layer. However, excessive use of the antistatic agent may lead to excessive surface moisture, potentially causing issues such as reduced long-term storage stability due to surface oxidation or a decrease in heat generation. Therefore, optimizing the amount of antistatic agent is necessary.

4. Conclusion

To reduce the incomplete combustion rate of Al powder, the aluminum oxide layer on the surface of Al powder was replaced with PTFE. DSC analysis showed a successful doubling of heat release; however, the electrostatic force on the powder surface increased by up to 20 times as an unintended side effect. To prevent spontaneous ignition due to static electricity, we explored antistatic agents capable of reducing electrostatic force and selected non-toxic chemicals, glycerol and Bis-Hydroxyethyl Cocomonium Nitrate. The reduction in electrostatic force was attributed to the formation of a conductive surface layer on the PTFE/Al powder, achieved through the absorption of moisture and trace amounts of salt by glycerol and Bis-Hydroxyethyl Cocomonium Nitrate. The higher polarity of Bis-Hydroxyethyl Cocomonium Nitrate enhances moisture and salt absorption, further decreasing the resistivity of the conductive layer and improving antistatic performance. Notably, Bis-Hydroxyethyl Cocomonium Nitrate demonstrated excellent efficiency in reducing electrostatic force with the addition of only a 0.05 wt.% concentration. As a result, treating PTFE/Al powder with a solution of 5 wt.% glycerol and 0.05 wt.% Bis-Hydroxyethyl Cocomonium Nitrate led to a 61% reduction in electrostatic force. However, overusing the antistatic agent might cause excessive surface moisture, potentially leading to issues such as decreased long-term storage stability due to surface oxidation or a reduction in heat generation. Therefore, optimizing the amount of antistatic agent is crucial. In conclusion, adjusting the proportion of antistatic agents further holds potential for significantly reducing electrostatic force in future applications.

Acknowledgement

This research was supported by a grant from the Korean Ministry of Trade, Industry, and Energy (Project No.: RS-2024-00467968).

REFERENCES

- [1] D.T. Osborne, et al., Effect of Al Particle Size on the Thermal Degradation of Al/Teflon Mixtures. Combust. Sci. Technol. **179**, 1467-1480 (2007).
 - DOI: https://doi.org/10.1080/00102200601182333
- [2] D.W. Kim, et al., Synergetic enhancement in the reactivity and stability of surface-oxide-free fine Al particles covered with a polytetrafluoroethylene nanolayer. Sci. Rep. 10, 14560 (2020). DOI: https://doi.org/10.1038/s41598-020-71162-z
- [3] K.S. Kappagantula, et al., Tuning Energetic Material Reactivity Using Surface Functionalization of Aluminum Fuels. J. Phys. Chem. C. 116, 24469-24475 (2012). DOI: https://doi.org/10.1021/jp308620t
- [4] Y. Lim, Fabrication and Characterization of Highly Reactive Al/ CuO Nano-composite using Graphene Oxide. J. Korean Powder Metall. Inst. 26, 220-224 (2019).
 - DOI: https://doi.org/10.4150/kpmi.2019.26.3.220
- [5] D.W. Kim, et al., Influence of poly(vinylidene fluoride) coating layer on exothermic reactivity and stability of fine aluminum particles. Appl. Surf. Sci. 551, (2021). DOI: https://doi.org/10.1016/j.apsusc.2021.149431
- [6] S.-H. Jung, et al., Increased exothermic reactivity of polytetrafluoroethylene-coated aluminum powders: Impact of powder size reduction. Mater. Lett. 351, (2023).
 - DOI: https://doi.org/10.1016/j.matlet.2023.135009

 R. Zhang, et al., Material choices for triboelectric nanogenerators:
- A critical review. EcoMat, **2**, (2020).

 DOI: https://doi.org/10.1002/eom2.12062
- [8] Z.B. Li, et al., Small-Sized, Lightweight, and Flexible Triboelectric Nanogenerator Enhanced by PTFE/PDMS Nanocomposite Electret. ACS Appl. Mater. Interfaces 11, 20370-20377 (2019). DOI: https://doi.org/10.1021/acsami.9b04321
- [9] Y. Ding, et al., Antistatic ability of 1-n-tetradecyl-3-methylimidazolium bromide and its effects on the structure and properties of polypropylene. Eur. Polym. J. 44, 1247-1251 (2008).
 DOI: https://doi.org/10.1016/j.eurpolymj.2008.01.030
- [10] Adriana, et al., Antistatic effect of glycerol monostearate on volume resistivity and mechanical properties of nanocomposite polystyrene-nanocrystal cellulose. AIP Conf. Proc. 1977, (2018). DOI: https://doi.org/10.1063/1.5042967
- [11] X. Zhang, et al., Effect of polyamide 6 on the morphology and electrical conductivity of carbon black-filled polypropylene composites. R. Soc. Open Sci. 4, 170769 (2017). DOI: https://doi.org/10.1098/rsos.170769
- [12] R. Ram, et al., Electrical and thermal conductivity of polyvinylidene fluoride (PVDF) Conducting Carbon Black (CCB) composites: Validation of various theoretical models. Compos. Part B Eng. 185, (2020).
 - DOI: https://doi.org/10.1016/j.compositesb.2020.107748
- [13] A. Tsurumaki, et al., Evaluation of ionic liquids as novel antistatic agents for polymethacrylates. Electrochim. Acta **248**, 556-561 (2017). DOI: https://doi.org/10.1016/j.electacta.2017.07.181
- [14] L. Wang, et al., A facile and industrially feasible one-pot approach to prepare graphene-decorated PVC particles and their application

- in multifunctional PVC/graphene composites with segregated structure. Compos. Part B Eng. **185**, (2020).
- DOI: https://doi.org/10.1016/j.compositesb.2020.107775
- [15] S. Salsabila, et al., Formulation of mono-diacylglycerol from palm fatty acid distillate and glycerol as antistatic agents on plastics. IOP Conf. Ser.: Earth Environ. Sci. 749, (2021). DOI: https://doi.org/10.1088/1755-1315/749/1/012069
- [16] C. Xing, et al., Ionic liquid modified poly(vinylidene fluoride): crystalline structures, miscibility, and physical properties. Polym. Chem. 4, (2013). DOI: https://doi.org/10.1039/c3py00466j
- [17] X. Wang, et al., Synthesis of non-destructive amido group functionalized multi-walled carbon nanotubes and their application in antistatic and thermal conductive polyetherimide matrix nanocomposites. Polym. Adv. Technol. 28, 791-796 (2017). DOI: https://doi.org/10.1002/pat.3979
- [18] C. Xing, et al., Toward an Optically Transparent, Antielectrostatic, and Robust Polymer Composite: Morphology and Properties of Polycarbonate/Ionic Liquid Composites. Ind. Eng. Chem. Res. 53, 4304-4311 (2014). DOI: https://doi.org/10.1021/ie404096b
- [19] T. Huang, et al., Carbon nanotubes induced microstructure and property changes of polycarbonate/poly(butylene terephthalate) blend. Compos. Part B Eng. 133, 177-184 (2018). DOI: https://doi.org/10.1016/j.compositesb.2017.09.037

- [20] G. Sun, et al., Fabrication and mechanical, electrical properties study of isocyanate-based polyimide films modified by reduced graphene oxide. Prog. Org. Coat. 143, (2020). DOI: https://doi.org/10.1016/j.porgcoat.2020.105611
- [21] F.J. Okparaocha, et al., Morphology and functional properties of electrospun expanded polystyrene (EPS)/reduced graphene oxide (RGO) nanofiber composite. Fullerenes Nanotubes Carbon Nanostruct. 27, 939-946 (2019).
 - DOI: https://doi.org/10.1080/1536383x.2019.1666365
- [22] Y. Tian, et al., Preparation of carbon nanotubes/polyethersulfone antistatic composite materials by a mixing process. Polym. Compos. 41, 556-563 (2019).
 - DOI: https://doi.org/10.1002/pc.25387
- [23] D.I. Arun, et al., Experimental and Monte Carlo simulation studies on percolation behaviour of a shape memory polyurethane carbon black nanocomposite. Smart Mater. Struct. 28, (2019). DOI: https://doi.org/10.1088/1361-665X/ab083b
- [24] X. Liang, et al., Waterborne polyurethane-acrylate-polyaniline: Interfacial hydrogen bonding for enhancing the antistatic, damping, and mechanical properties. Polym. Adv. Technol. 33, 2667-2681 (2022). DOI: https://doi.org/10.1002/pat.5722
- [25] https://www.bondline.co.uk/product/esd-sprays-and-cleaning/anti-static-general-purpose-staticide-spray, accessed 20.03.2025